Published in final edited form as:
*Cell Oncol (Dordr)*. 2013 June ; 36(3): 247–257. doi:10.1007/s13402-013-0132-x.

# Composite fatty acid ether amides suppress growth of liver cancer cells in vitro and in an in vivo allograft mouse model

**Mengde Cao**,
Banyan Laboratories, Inc., Alachua, FL 32615, USA

**Victor Prima**,
Banyan Laboratories, Inc., Alachua, FL 32615, USA

**David Nelson**, and
Division of Gastroenterology, Hepatology, and Nutrition, University of Florida, Gainesville, FL 32610, USA

**Stanislav Svetlov**
Banyan Laboratories, Inc., Alachua, FL 32615, USA

Department of Medicine, University of Florida, Gainesville, FL 32610, USA

Mengde Cao: mcao@banyanbio.com; Stanislav Svetlov: ssvetlov@banyanbio.com

## Abstract

**Background—**The heterogeneity of liver cancer, in particular hepatocellular carcinoma (HCC), portrays the requirement of multiple targets for both its treatment and prevention. Multi-faceted agents, minimally or non-toxic for normal hepatocytes, are required to address the molecular diversity of HCC, including the resistance of putative liver cancer stem cells to chemotherapy.

**Methods—**We designed and synthesized two fatty acid ethers of isopropylamino propanol, C16:0-AIP-1 and C18:1-AIP-2 (jointly named AIPs), and evaluated their anti-proliferative effects on the human HCC cell line Huh7 and the murine hepatoma cell line BNL 1MEA.7R.1, both in vitro and in an in vivo allograft mouse model.

**Results—**We found that AIP-1 and AIP-2 inhibited proliferation and caused cell death in both Huh7 and BNL 1MEA.7R.1 cells. Importantly, AIP-1 and AIP-2 were found to block the activation of putative liver cancer stem cells as manifested by suppression of clonal ‘carcinosphere’ development in growth factor-free and anchorage-free medium. The AIPs exhibited a relatively low toxicity against normal human or rat hepatocytes in primary cultures. In addition, we found that the AIPs utilized multifaceted pathways that mediate both autophagy and apoptosis in HCC, including the inhibition of AKTs and CAMK-1. In immune-competent mice, the AIPs significantly reduced BNL 1MEA.7R.1 cell-driven tumor allograft development, with a higher efficiency than sorafenib. A combination of AIP-1 + AIP-2 was most effective in reducing the tumor allograft incidence.

**Conclusions—**AIPs represent a novel class of simple fatty acid derivatives that are effective against liver tumors via diverse pathways. They show a low toxicity towards normal hepatocytes. The addition of AIPs may represent a new avenue towards the management of chronic liver injury and, ultimately, the prevention and treatment of HCC.



Correspondence to: Mengde Cao, mcao@banyanbio.com; Stanislav Svetlov, ssvetlov@banyanbio.com.

**Keywords**

Hepatocellular carcinoma (HCC); Alkyl (alkenyl)oxy-isopropylamino propanol (AIP); beta-spectrin; Autophagy; Apoptosis; AKT; Tumor allograft

## 1 Introduction

In spite of the progress that has been made in cancer treatment in recent years, many tumors remain refractory or relapse following an initial remission. Accumulating evidence suggests that cancer stem cells (CSCs) may be responsible, not only for tumor initiation and progression, but also for drug resistance and relapse. CSCs possess stem cell properties, such as the ability of self renewal, and have been identified in several types of cancer including liver cancer. Current conventional chemotherapy regimens suffer from two significant problems: non-selective cytotoxicity (acting on both diseased and healthy cells) and non-anti-renewal capacity. Whereas most conventional chemotherapeutic drugs are able to eradicate the bulk of the tumor cells, they seem to be ineffective against CSCs and, thereby, ineffective in eradicating the 'root of the problem' [1–3]. Hence, the development of novel compounds targeting CSCs in heterogeneous tumor masses is becoming increasingly important for the ultimate treatment of cancer.

Liver cancer, particularly hepatocellular carcinoma (HCC), is the fifth most common cancer worldwide [4] and it ranks third in morbidity and mortality. Despite the approval and extensive clinical application of sorafenib in the treatment of HCC, the prognosis for patients with advanced HCC has remained poor and the benefits of sorafenib in this group have remained modest. In addition, a relatively high toxicity and various side effects significantly limit its use [5–7]. Thus, improving the overall survival of patients with advanced HCC requires the development of a more effective systemic therapy.

Liver cancer in general, and HCC in particular, is a very heterogeneous disease with a variety of molecular mechanisms underlying both its initiation and progression. This notion highlights the need to identify multiple 'targets' for both HCC prevention and treatment [8]. To overcome the complexity of molecular (genomic and epigenomic) aberrations in HCC, combination therapies aimed at resolving the underlying conditions, such cirrhosis of the liver, will be critical. Multi-faceted drugs, non-toxic for residual normal hepatocytes, are required to overcome this molecular complexity, including the resistance of putative cancer stem/progenitor cells to chemotherapy. In the present study, we designed and synthesized two novel fatty acid derivatives of isopropylamino propanol (jointly named AIPs), and evaluated their antitumor effects on human and murine liver tumor cell lines in vitro and in vivo. Our results indicate that the addition of AIPs may provide a new avenue towards the treatment, and particularly the prevention, of HCC.

## 2 Materials and methods

### 2.1 Synthesis and purification of AIPs

**Synthesis of 3-alkyloxy(3-alkenyloxy)-1,2-epoxypropanes (Fig. 1; Fig. 2a, b)—** 1a, b (10 mmol) in 20 mL of dry THF was added under $N_2$ to a stirred suspension of NaH (10 mmol) at 5–10 °C and the mixture was stirred at 22 °C (room temperature, rt) for 1 h. Next, epichlorohydrin (20 mmol) was added and the mixture was heated at reflux for 2.5–4 h. After evaporation and extraction with EtOAc (3×35 mL) the product was purified by chromatography to give 2a, b with 64 % and 47 % yields, respectively (Fig. 1).

**Synthesis of 1-alkyloxy(1-alkenyloxy)-3-isopropylamino-propan-2-oles (3a, b)—**Oxirane (2a, b) (4 mmol) and isopropylamine (32 mmol) in 2-propanol (40 mL) was stirred at 50–55 °C for 7–8 h. After solvent evaporation the residue was purified by re-crystallization or chromatography to obtain pure hexadecyl-AIP-1 (3a, mp 55– 57 °C) and octadecenyl-AIP-2 (3b, colorless oil) in 83 % and 86 % yields, respectively. The chemical structure of the AIP-bases was confirmed by NMR and mass spectrometry (Fig. 1b).

**Preparation of 1-alkyloxy(1-alkenyloxy)-3-isopropylamino-propan-2-olhydrochlorides (4a, b)—**1-Alkyloxy(1-alkenyloxy)-AIP (3a, b) (2 mmol) was dissolved in ether (35 mL) and HCl (4 mmol, 2 M in ether) was added drop-wise at 5–10 °C with stirring. The solid phase was filtered after 0.5 h at room temperature and washed with ether for (4a), or the solvent was evaporated for (4b) to yield pure C16-AIP-1-HCl (4a) (91 %, white micro-crystals, mp 75–77 °C) or C18-AIP-2-HCl (4b) (97 %, yellowish oil).

## 2.2 Cell culture and reagents

The human hepatocellular carcinoma (HCC) cell line Huh7 was obtained from Dr. Chen Liu, Department of Pathology, Immunology and Laboratory Medicine, University of Florida. The murine liver hepatoma cell line BNL 1MEA.7R.1 was obtained from the American Type Culture Collection (referred as 1MEA in this study) (ATCC, Manassas, VA). In strict accordance with the supplier's instructions and established procedures, all cell lines were maintained in Dulbecco's minimal essential medium (DMEM) supplemented with 10 % heat-inactivated fetal bovine serum (FBS) (GIBCO) and 100 U/ml penicillin, 100 μg/ml streptomycin (Cellgro), L-glutamine (2 mM) in a humidified atmosphere of 5 % $CO_2$ at 37 °C. Normal primary human hepatocytes were obtained from ADMET Technologies and cultured in DMEM/F12 (1:1) medium containing 10 % FBS, supplemented with insulin-transferrin-selenium (Invitrogen, Inc.) and dexameth-asone (40 ng/ml). The normal human hepatocytes used were at least 90 % viable before treatment. Anti-caspase 3, anti-caspase 7, anti-caspase 9, anti-PARP, anti-phospho-AKT, anti-AKT, and anti-survivin antibodies were obtained from Cell Signaling Technology (Beverly, MA). Anti-LC3 was purchased from Novus Biologicals, anti-beta-spectrin from BD Biosciences, and goat anti-rabbit or anti-mouse alkaline phosphatase (AP)-conjugated secondary antibodies were purchased from EMD Biosciences.

## 2.3 Cell viability assay

Cell viability was determined using the CellTiter 96® $AQ_{ueous}$ non-radioactive cell proliferation assay kit (Promega, Madison WI, USA) according to the manufacturer's instructions. Briefly, the Huh7 and 1MEA cell lines were seeded in 96-well plates (Costar) at $1\times10^4$ cells per well and cultured in DMEM with 10 % FBS. Twelve hours later, cells were treated with different doses of AIP-1, AIP-2 or DMSO as a control (less than 0.1 %, v/v) for another 24 h. At the end of the incubation period, 20 μl of the combined MTS/PMS solution was added to each well. Following 4 h of incubation at 37 °C and 5 % CO2, MTS will be reduced by the living cells into a formazan product whose quantity is directly proportional to the number of cells in culture. The amount of formazan product was measured at 490 nm absorbance. The results are presented as means ± SD from three independent experiments. Inhibition graphs were plotted using mean values obtained from each concentration relative to control values.

## 2.4 Carcinosphere formation assay

Huh7 cells were grown as indicated above until sub-confluency, then gently trypsinized, collected and washed with PBS. Next, the cells were re-suspended in a small volume of serum-free DMEM/F12 medium, triturated and verified visually to contain only single cells,

and counted in a hemocytometer. The cells were seeded in 6-well plates ($5\times 10^4$ cells/well) in serum-free DMEM/F12, 1:1 supplemented with 0.8 % methylcellulose (MC), followed by the addition of AIPs at different concentrations (1–25 μM). The formation of spheroids was observed under an inverted-phase microscope ~96 h after plating. The size and the number of carcinospheriods per well were counted after 14 days using a phase contrast microscope equipped with morphometric analysis software at ×20 magnification. Data are shown as means ± SD of values from triplicate experiments.

### 2.5 Kinase activity assays

AKTs, CAMK-1, SPHK2 and several other kinases were measured in 96-well ELISA plates according to the Adapta and Z-Lite assay protocols (Invitrogen). Briefly, for AKT the final 10 μL Kinase Reaction mixture consisted of 1–40 ng AKT-1, −2 or −3 and 2 μM Ser/Thr 06 in 50 mM HEPES pH 7.5, 0.01 % BRIJ-35, 10 mM MgCl2, 1 mM EGTA. AIPs were added prior to the addition of substrates. After a 1 h Kinase Reaction incubation, 5 μL of a 1:2048 dilution of Development Reagent A was added, and fluorescence was measured according to manufacturer's protocol (Invitrogen). For CAMK-1, the final 10 μL Kinase Reaction mixture consisted of 3.75–25 ng CAMK-1 and 200 μM ZIPtide in 32.5 mM HEPES pH 7.5, 0.005 % BRIJ-35, 5 mM MgCl2, 2 mMCaCl2,20 μg/ml Calmodulin, 100 μM ATP and 0.01 % NaN3. In the SPHK2 assay, the Kinase Reaction mixture contained 25–134 ng SPHK2 and 50 μM Sphingosine Lipid Substrate in 32.5 mM HEPES pH 7.5, 0.5 mM EGTA, 1.5 mM MgCl2 and 100 μM ATP. AIPs were added at the desired concentrations before addition of the substrates. After a 1 h Kinase Reaction incubation, 5 μL of Detection Mix was added and fluorescence was measured according to manufacturer's protocol. $IC_{50}$ values were determined from the results of at least three independent experiments and calculated by the Logit method.

### 2.6 Western blot analysis

Cells were harvested and washed twice with 1× PBS and prepared for sodium dodecyl sulfate-polyacrylamide gel electrophoresis (SDS-PAGE). Briefly, cell pellets were re-suspended in RIPA buffer (Thermo Scientific) supplemented with 1 % EDTA (0.5 M), phosphatase inhibitor cocktail 1 and 2 (Sigma) and Protease Arrest ™ (G Biosciences) and incubated on ice for 30 min. After centrifugation at 12,000×g at 4 °C for 15 min, the supernatant was transferred to a new tube and the protein concentration was determined using a BCA™ Protein Assay Kit (Thermo Scientific). Twenty micrograms (20 μg) of protein per lane were subjected to SDS-PAGE on Tris/glycine gels (Millipore, Billerica, MA, USA) at 120 V for 2 h. Next, the separated proteins were laterally transferred to polyvinylidene fluoride (PVDF) membranes in a transfer buffer at a constant voltage of 20 V for 2 h at ambient temperature in a semi-dry transfer unit (Bio-Rad, Hercules, CA, USA). After electro-transfer, the membranes were blocked for 1 h at ambient temperature in 5 % non-fat milk in TBS and 0.05 % Tween-2 (TBST), and then incubated with primary antibodies in TBST with 5 % non-fat milk at 1:1000 dilution at 4 °C overnight. This incubation was followed by three washes with TBST and a 1 hour incubation at ambient temperature with a secondary antibody-conjugated alkaline phosphatase. Immunoreactive bands were detected using a BCIP/NBT reagent (KPL, Rockville, MD, USA). The molecular sizes of the proteins detected were determined using pre-stained Full-Rrange Rainbow Molecular Weight Markers (GE Health, NJ).

### 2.7 Tumor allograft and AIPs treatment

BALB/c mice (6–8 weeks of age) were obtained from the Jackson Laboratory. The mice were kept under pathogen-free conditions, and food and water were supplied ad libitum. Housing and all procedures involving animals were performed according to protocols approved by the animal care and use committee, in accordance with the requirements of the

Institutional Guideline for Animal Experiments. The right flanks of the mice were injected subcutaneously (s.c.) with $5\times10^6$ 1MEA cells in 100 μl of phosphate-buffered saline (PBS). After one week, the injected mice were randomly divided into five groups (5 mice/group) and orally fed with AIP-1, AIP-2, AIP-1 + AIP-2 (25 mg/kg), or Sorafenib (30 mg/kg), or 100 μ1. PBS (control group), respectively, once daily for 5 days weekly, by gavage for 4 weeks. At the end of the experiments, the mice were sacrificed and the tumors were recovered and weighed as described previously [9]. The tumor sizes were indicated as weight (mg).

### 2.8 Statistical analysis

The statistical significance between values was determined by Student's *t*-test. All data were expressed as the mean ± SD. Probability values of $P \leq 0.05$ were considered significant.

## 3 Results

### 3.1 AIP-1 and AIP-2 inhibit growth of Huh7 and 1MEA cells, but not of normal human hepatocytes

The AIP compounds were synthesized as described under 'Section 2', and its schematic chemical structures, synthesis procedures and mass spectra are depicted in Fig. 1. We first determined the inhibitory effects of the AIP compounds at different concentrations on the proliferation and viability of human hepatocellular carcinoma cells (Huh7), murine hepatoma cells (1MEA) and normal human hepatocytes using the MTS assay as outlined under 'Section 2'. By doing so, we found that AIP-1 and AIP-2 have the capability to inhibit proliferation of both Huh7 (Fig. 2a and d) and 1MEA (Fig. 2b) cancer cells in a dose-dependent manner, but not of normal human hepatocytes (Fig. 2c and e). As compared to controls, we found that AIP-1 did (at a dose of 20 μM) significantly inhibit Huh7 cell growth (Fig. 2d), but at a similar dose did not cause toxicity in normal human primary hepatocytes (Fig. 2e). Taken together, these results suggest that the AIP compounds are selectively toxic to liver cancer cells.

### 3.2 AIPs suppress Huh7 carcinopheroid formation

HCC progression has been thought to be driven by CSCs through their capacity of self-renewal, production of heterogeneous progeny, resistance to chemotherapy, and ability of unlimited division [10]. A successful eradication of cancer requires anticancer therapy that affects both the bulk of cancer cells and the putative, relatively small, CSC population [11, 12] and that, at the same time, avoids toxic side effects for other normal cell types. To this end, we examined the inhibitory action of AIP-1 against carcinospheriod formation (see 'Section 2') of Huh7 cells in serum-free and anchorage-free methylcellulose medium. By doing so, we found that, compared to the untreated control, AIP-1 significantly inhibited Huh7 carcinoshphere formation (Fig. 3), thereby suggesting that AIP-1 can remove the 'seed' cells (CSC) present in the Huh7 cell population.

### 3.3 AIP-1 and AIP-2 inhibit multiple kinase activities in cell-free and intact cell systems

Deregulation of protein kinases and its concomitant signaling pathways is commonly observed in cancer cells, thereby turning these kinases into attractive targets for the design of anticancer drugs [13]. Accordingly, we tested whether the novel AIP compounds synthesized here possess inhibitory activities towards the protein kinases AKT-2, CAMK-1 and SPHK2 in a cell-free system. Through this test, we found that both AIP compounds potently inhibited the kinases mentioned (Fig. 4a–c). When compared at the same doses, AIP-2 had a relatively stronger inhibitory effect than AIP-1 on these protein kinases in the cell-free system used. We next determined the inhibitory activities of AIP-1 and AIP-2 on

the phosphorylation and expression of AKT and CAMK-1 at the cellular level. As shown in Fig. 4d, AIP-1 significantly inhibited, and AIP-2 only slightly inhibited, CAMK-1 expression in Huh7 cells. Similarly, AIP-1 effectively inhibited the phosphorylation of AKT in Huh7 cells at a dose of 10 μM, whereas both AIPs had no obvious inhibitory effect on AKT expression.

### 3.4 AIP-1 down-regulates survivin, activates autophagy and apoptosis, and promotes beta-spectrin degradation in Huh7 and 1MEA cells

Accumulating evidence suggests that survivin promotes cell survival, inhibits cell apoptosis, and regulates cancer cell autophagy [14]. The above observations prompted us to evaluate the effects of both AIP compounds on survivin expression and its concomitant effects on apoptosis and autophagy, and on the expression of the cytoskeletal protein beta-spectrin in Huh7 and 1MEA cells. Compared to the untreated controls, AIP-1 and AIP-2 were found to significantly down-regulate survivin expression (top panel in Fig. 5a and b), and to up-regulate the expression of the autophagy-associated protein LC3-II (second panel in Fig. 5a and b) in both Huh7 (Fig. 5a) and 1MEA (Fig. 5b) cells in a dose-dependent manner. In contrast, the two AIPs had different effects on the expression of several apoptosis-associated proteins such as cleaved caspase 3, cleaved caspase 7, cleaved caspase 9 and cleaved PARP in both Huh7 (Fig. 5a) and 1MEA (Fig. 5b) cells. AIP-1 significantly up-regulated cleaved caspase 7, cleaved caspase 9 and cleaved PARP expression, whereas AIP-2 only slightly enhanced the expression of cleaved caspase 9 and cleaved PARP at a high dose (10 μM) in Huh7 cells (Fig. 5a). AIP-1 increased cleaved caspase 3 and cleaved PARP expression in 1MEA cells, whereas no changes were observed in cleaved caspase 3, cleaved caspase 7 and cleaved PARP expression in 1MEA cells treated with AIP-2 (Fig. 5b).

As major components of the cytoskeletal network associated with the plasma membrane of vertebrate cells, different spectrin isoforms serve as potential targets for both calpain and caspase actions during cell morphology changes and apoptosis. Previous studies have shown that β2 spectrin plays a crucial role in the pathogenesis of liver fibrosis and the development of hepatocellular carcinoma [15–17]. Based on this notion and our above observations, we next examined whether the two AIP compounds can induce spectrin breakdown product (BDP) formation in our tested cancer cell lines. By doing so, we found that treatment of Hu7 cells with AIP-1 (Fig. 5c, lanes 2–4) dose-dependently promoted cleavage of β II spectrin into βII-BDP110 and βII-BDP85 fragments, whereas AIP-2 (lanes 5–7) was only able to induce βII-BDP85 fragments. To further assess a correlation between the occurrence of multiple βII-BDPs and the activity of calpains and caspases, Huh7 and 1MEA cells were treated with AIP-1 at a dose of 10 (μM, with or without 30 min of pretreatment with either the calpain inhibitor SNJ1945, the caspase3 inhibitor BT-1103, or the caspase 3 activator EDTA. Compared to the untreated controls (Fig. 5d, lane 1), 1MEA (upper panel) and Huh7 (lower panel) cells treated with AIP-1 showed increases in the levels of βII-BDP110 and βII-BDP85 (Fig. 5d, lane 2). We also found that the production of βII-BDP85 strikingly paralleled the activity of caspase 3 (Fig. 5d, lanes 6–8). Pretreatment with the calpain inhibitor SNJ1945 did not block βII-BDP85 formation in Huh7 and 1MEA cells (Fig. 5d, lanes 3–5). However, the caspase inhibitor BT-1103 successfully blocked βII-BDP85 formation in both pretreated cells and down-regulated the βII-BDP110 levels in 1MEA cells (Fig. 5d, lanes 6–8), whereas the caspase activator EDTA increased the levels of βII-BDP85 in both cell lines (Fig. 5d, lane 9). No changes were observed on αII spectrin expression in the cells tested (data not shown). Taken together, these results suggest that caspases can mediate βII spectrin cleavage in Huh7 and 1MEA cells treated with AIP-1 at the doses indicated.

### 3.5 AIPs decrease tumor incidence and inhibit tumor growth in vivo

To next investigate whether AIPs can affect tumor growth in vivo, we employed an allograft model of 1MEA cells in immune-competent mice as reported previously [9]. Tumor allografts were palpable after ~2 weeks in all mice injected with $5 \times 10^6$ 1MEA cells, and 4 weeks after inoculation all non-treated mice developed visible and measurable tumors (Fig. 6a). A 4 week treatment with AIP-2 alone or with a combination of AIP-1 + AIP-2 significantly reduced the number of tumor-bearing mice, i.e., 40 % of the mice treated with AIP-2 and 20% of the mice treated with AIP-1 + AIP-2 did not show any signs of tumor formation. Treatment of the mice with sorafenib delayed tumor development (i.e., relatively small tumor sizes), but did not decrease the tumor incidence in 1MEA inoculated mice. In contrast, the combination treatment of AIP-1 + AIP-2 not only significantly inhibited tumor growth, but also slightly decreased the tumor incidence (Fig. 6).

## 4 Discussion

Treatment, and also chemo-preventive, options for hepatocellular carcinoma (HCC) patients are currently limited. The main problem with chemotherapy or chemoprevention of HCC is that most patients suffer from an underlying cirrhosis and that, as such, cytotoxic therapy can easily kill the few remaining normal functional hepatocytes [18]. Even with the current reference criterion treatment of sorafenib, which has modest survival advantages, all patients eventually progress due to either non-responsiveness, early resistance or intolerance [7]. Up to 90 % of the patients receiving this drug have been reported to develop dermatological symptoms [8]. This situation highlights the urgent need for the design of novel drugs and HCC treatment/prevention strategies. In the present study, we developed two novel fatty acid ether amides (AIPs) as experimental anti-cancer drugs for the treatment and prevention of liver cancer, and assessed their cytotoxicity in vitro in liver cancer-derived cell lines and normal human primary hepatocytes, and in an in vivo allograft model. Our results clearly indicate that the AIPs developed exhibit anti-proliferative and cytotoxic effects on human hepatocelluar carcinoma Huh7 cells and murine hepatoma 1MEA cells, but not on normal human primary hepatocytes.

Recently, cancer stem cells (CSCs) have attracted attention as novel therapeutic targets for liver cancer, and evidence is accumulating that CSC properties, such as self-renewal and unlimited proliferation, are highly relevant to the development, recurrence and drug resistance of HCC [19, 20]. However, conventional anticancer therapies, including chemotherapy, radiation and immunotherapy, preferentially kill rapidly growing tumor cells, thereby reducing the tumor mass but, at the same time, leaving relatively slow growing cancer-initiating cells (CSCs) unaffected. This might ultimately result in relapse and the proliferation of therapy-resistant and more aggressive tumor cells. Thus, the development of a specific CSC-based therapy might be a strategy to overcome the high recurrence rate of HCC [11]. In this study, we have shown that AIP-1, even at a low concentration of 1 μM, can significantly inhibit Huh7 carcinospheroid formation under serum-free and anchorage-free culture conditions. This result suggests that the AIP compounds may have strong anti-renewal abilities and may remove the ‘seed’ CSCs present in the Huh7 cell line.

The (de)regulation of specific protein kinases, and apoptosis and autophagy pathways, is known to play an important role in the initiation and progression of cancer, and the targeting of these pathways has emerged as an attractive approach for the treatment of various cancers [21–23]. Our kinase activity assays in cell-free and intact Huh7 cells have shown that both AIP-1 and AIP-2 can inhibit the activities of multiple kinases, including AKT, CAMK-1 and SPHK2, in a dose-dependent manner. The PI3K/AKT/mTOR pathway plays a critical role in the pathogenesis of HCC and the level of AKT is frequently up-regulated in various cancers to maintain tumor cell survival and growth [24, 25]. Based on these data, we hypothesized

that the observed inhibition of HCC cell proliferation by the AIP compounds might be associated with a (de)regulation of the PI3K/AKT/mTOR pathway. Indeed, our results showed that AIP-1 and AIP-2 inhibited the activity and phosphorylation of AKT, but not that of total AKT protein expression. Taken together, these data suggest that the AIP compounds developed may inhibit cell proliferation by blocking multiple kinase activities in HCCs.

Based on our above results, we further assessed putative mechanisms underlying the anti-proliferative and anti-renewal capacities of the AIP compounds observed, including survivin, and autophagy- and apoptosis-associated protein expression. Survivin is a member of the inhibitors-of-apoptosis protein (IAPs) family. At the clinical level, it has been shown that survivin expression is up-regulated in various human cancers, including liver cancer, and that its up-regulation is associated with tumor resistance to both chemotherapy and radiation therapy [26, 27]. In this study, we examined the effects of AIP compounds on survivin expression in Huh7 and 1MEA cells. By doing so we found, for the first time, that the AIP compounds could significantly down-regulate survivin expression in these cells in a dose-dependent manner. Because of the involvement of autophagy in many disease conditions, there is great interest in identifying drugs that can be used to manipulate autophagy for therapeutic purposes. The autophagy lyso-somal pathway is one of the targets that is being explored in multiple cancers, including HCC, and may serve as a promising avenue for further therapeutic development [28]. Autophagic cell death, or type II programmed cell death, is distinct from type I programmed cell death (apoptosis), which is also implicated in cancer development [29]. In the present study, we harvested all cells, including floating cells, after a 24 h treatment with AIP compounds to assess autophagy by Western blotting. We found that the expression of the autophagy marker protein LC3-II was significantly increased in AIP compound-treated Huh7 and 1MEA cells as compared to untreated controls. No changes in LC3-I levels were observed following AIP treatment, as determined by Western blotting. This result suggests that a pool of LC3-II protein may be generated following AIP exposure, that is translocated to the outer membrane of the autophagosomes. Our results indicate that both AIP-1 and AIP-2 can induce autophagy in human and murine liver cancer cells.

Caspases are essential in the initiation and progression of apoptosis [30], and they account for the majority of cellular and morphological events that occur during cell death [31, 32]. Here, we show that AIP-1 and AIP-2 can induce apoptosis in Huh7 and 1MEA cells through activating caspases and other apoptosis-associated proteins. Specifically, we found that AIP-1 and AIP-2 can increase active caspase 7, caspase 9, and PARP levels in Huh7 cells, and active caspase 3, caspase 7, and PARP levels in 1MEA cells. Apoptosis and autophagy are two distinct forms of programmed cell death [30] that may be interconnected or even simultaneously induced by the same stimulus, resulting in different cellular outcomes [31, 32]. We found, for the first time, that the two AIP compounds can induce both apoptosis and autophagy in Huh7 and 1MEA cells. Cancer cells may evade apoptosis to support malignant growth, while traditional cancer therapies mainly focus on enhancing apoptosis [33]. Some reports have suggested that anti-cancer treatment inhibits the killing of tumor cells by inducing autophagy, whereas other reports have proposed that autophagy is a cell death mechanism that can function as a collaborator of apoptosis or as a back-up when apoptosis has become ineffective [34]. Taken together, our results suggest that the anti-proliferative effects of the AIP compounds are associated with autophagy and apoptosis induction in Huh7 and 1MEA cells. Further work is needed to unravel the exact relationship between these two cell-death pathways in the context of AIP compounds.

Spectrin is the major component of the cytoskeletal network, and calpain-mediated cleavage of spectrin has been observed during apoptosis in U937 cells [35] and in neurons [36, 37].

However, accumulating evidence indicates that αII spectrin cleavage in itself is not lethal to the cell [38], and it has been suggested that when spectrin is cleaved by caspase 3 during apoptosis the advent of βII subunit cleavage may mark an irreversible transition in the cortical cytoskeleton that may contribute to impaired cell viability [39]. Calpains and caspases are cysteine proteases that are ubiquitously expressed in vertebrate cells. Degradation of proteins by these two proteases is associated with many cellular processes, including cell motility and apoptosis [40]. We observed that Huh7 and 1MEA cells treated with AIP compounds exhibited different βII spectrin breakdown product (BDP) formation profiles. Compared to untreated controls, AIP-1 and AIP-2 treatment dose-dependently induced an increase in the level of βII-BDP85 fragment formation in Huh7 cells. We also found that the caspase 3 inhibitor BT1103, but not the caipain inhibitor SNJ1945, could block βII spectrin degradation. No αII spectrin cleavage was observed in the cells tested. Taken together, these results suggest that βII spectrin cleavage is mediated by caspases in Huh7 and 1MEA cells treated with AIP-1.

Finally, we evaluated the in vivo antitumor effects of AIPs on murine hepatoma 1MEA cells in an ectopic allograft model. Compared with sorafenib, AIP-2 alone and AIP-2 + AIP-1 were more effective in decreasing the tumor incidence in this model. In contrast, the AIP-1 + AIP-2 combination showed a tumor growth inhibition pattern similar to that of sorafenib in this adopted ectopic allograft model. Our in vivo data show that the combination therapy of AIP-1 + AIP-2 is not only more effective in decreasing the tumor incidence, but is also effective in significantly inhibiting tumor development when compared with sorafenib, which is currently considered as the reference criterion standard of systemic therapy for HCC patients.

In summary, our results show, for the first time, that AIP compounds possess antitumor activity in HCC cells. Importantly, the AIPs developed inhibited the growth of tumor cells but not that of normal hepatocytes. These findings suggest that AIP compounds may serve as potent oral drugs for HCC prevention and treatment.

## Acknowledgments

We would like to thank Dr. Anatoliy Vakulenko for his excellent technical support in the synthesis, purification, and preparation of the AIP compounds. We also thank Mr. Archie Svetlov for editing the paper.

## References

1. Prud'homme GJ. Cancer stem cells and novel targets for antitumor strategies. Curr. Pharm. Des. 2012; 18:2838–2849. [PubMed: 22390767]
2. Grotenhuis BA, Wijnhoven BP, van Lanschot JJ. Cancer stem cells and their potential implications for the treatment of solid tumors. J. Surg. Oncol. 2012; 106:209–215. [PubMed: 22371125]
3. Tong CM, Ma S, Guan XY. Biology of hepatic cancer stem cells. J. Gastroenterol. Hepatol. 2011; 26:1229–1237. [PubMed: 21557770]
4. Parkin DM, Bray F, Ferlay J, Pisani P. Estimating the world cancer burden: Globocan, 2000. Int. J. Cancer. 2001; 94:153–156. [PubMed: 11668491]
5. Bosch FX, Ribes J, Diaz M, Cleries R. Primary liver cancer: worldwide incidence and trends. Gastroenterology. 2004; 127:S5–S16. [PubMed: 15508102]
6. Llovet JM, Burroughs A, Bruix J. Hepatocellular carcinoma. Lancet. 2003; 362:1907–1917. [PubMed: 14667750]
7. Llovet JM, Ricci S, Mazzaferro V, Hilgard P, Gane E, Blanc JF, de Oliveira AC, Santoro A, Raoul JL, Forner A, Schwartz M, Porta C, Zeuzem S, Bolondi L, Greten TF, Galle PR, Seitz JF, Borbath I, Häussinger D, Giannaris T, Shan M, Moscovici M, Voliotis D, Bruix J. SHARP Investigators Study Group, Sorafenib in advanced hepatocellular carcinoma. N. Engl. J. Med. 2008; 359:378–390. [PubMed: 18650514]

8. Yang CH, Lin WC, Chuang CK, Chang YC, Pang ST, Lin YC, Kuo TT, Hsieh JJ, Chang JW. Hand-foot skin reaction in patients treated with sorafenib: a clinicopathological study of cutaneous manifestations due to multitargeted kinase inhibitor therapy. Br. J. Dermatol. 2008; 158:592–596. [PubMed: 18070211]
9. Cao M, Xu Y, Youn JI, Cabrera R, Zhang X, Gabrilovich D, Nelson DR, Liu C. Kinase inhibitor Sorafenib modulates immunosuppressive cell populations in a murine liver cancer model. Lab Invest. 2011; 91:598–608. [PubMed: 21321535]
10. Oishi N, Wang XW. Novel therapeutic strategies for targeting liver cancer stem cells. Int. J. Biol. Sci. 2011; 7:517–535. [PubMed: 21552419]
11. Klonisch T, Wiechec E, Hombach-Klonisch S, Ande SR, Wesselborg S, Schulze-Osthoff K, Los M. Cancer stem cell markers in common cancers - therapeutic implications. Trends Mol. Med. 2008; 14:450–460. [PubMed: 18775674]
12. Dingli D, Michor F. Successful therapy must eradicate cancer stem cells. Stem Cells. 2006; 24:2603–2610. [PubMed: 16931775]
13. Gossage L, Eisen T. Targeting multiple kinase pathways: a change in paradigm. Clin. Cancer Res. 2010; 16:1973–1978. [PubMed: 20215532]
14. Zhao X, Ogunwobi OO, Liu C. Survivin inhibition is critical for Bcl-2 inhibitor-induced apoptosis in hepatocellular carcinoma cells. PLoS One. 2011; 6:e21980. [PubMed: 21829603]
15. Baek HJ, Lim SC, Kitisin K, Jogunoori W, Tang Y, Marshall MB, Mishra B, Kim TH, Cho KH, Kim SS, Mishra L. Hepatocellular cancer arises from loss of transforming growth factor beta signaling adaptor protein embryonic liver fodrin through abnormal angiogenesis. Hepatology. 2008; 48:1128–1137. [PubMed: 18704924]
16. Tang Y, Kitisin K, Jogunoori W, Li C, Deng CX, Mueller SC, Ressom HW, Rashid A, He AR, Mendelson JS, Jessup JM, Shetty K, Zasloff M, Mishra B, Reddy EP, Johnson L, Mishra L. Progenitor/stem cells give rise to liver cancer due to aberrant TGF-beta and IL-6 signaling. Proc. Natl. Acad. Sci. U. S. A. 2008; 105:2445–2450. [PubMed: 18263735]
17. Wang Z, Liu F, Tu W, Chang Y, Yao J, Wu W, Jiang X, He X, Lin J, Song Y. Embryonic liver fodrin involved in hepatic stellate cell activation and formation of regenerative nodule in liver cirrhosis. J. Cell Mol. Med. 2012; 16:118–128. [PubMed: 21388516]
18. Rougier P, Mitry E, Barbare JC, Taieb J. >Hepatocellular carcinoma (HCC): an update. Semin. Oncol. 2007; 34:S12–S20. [PubMed: 17449346]
19. Jordan CT, Guzman ML, Noble M. Cancer stem cells. N. Engl. J. Med. 2006; 355:1253–1261. [PubMed: 16990388]
20. Chiba T, Zheng YW, Kita K, Yokosuka O, Saisho H, Onodera M, Miyoshi H, Nakano M, Zen Y, Nakanuma Y, Nakauchi H, Iwama A, Taniguchi H. Enhanced self-renewal capability in hepatic stem/progenitor cells drives cancer initiation. Gastroenterology. 2007; 133:937–950. [PubMed: 17673212]
21. Ghobrial IM, Witzig TE, Adjei AA. Targeting apoptosis pathways in cancer therapy. CA Cancer J. Clin. 2005; 55:178–194. [PubMed: 15890640]
22. Senderowicz AM. Targeting cell cycle and apoptosis for the treatment of human malignancies. Curr. Opin. Cell Biol. 2004; 16:670–678. [PubMed: 15530779]
23. Cheng AL, Kang YK, Chen Z, Tsao CJ, Qin S, Kim JS, Luo R, Feng J, Ye S, Yang TS, Xu J, Sun Y, Liang H, Liu J, Wang J, Tak WY, Pan H, Burock K, Zou J, Voliotis D, Guan Z. Efficacy and safety of sorafenib in patients in the Asia-Pacific region with advanced hepatocellular carcinoma: a phase III randomised, double-blind, placebo-controlled trial. Lancet Oncol. 2009; 10:25–34. [PubMed: 19095497]
24. Bhaskar PT. N. Hay. The two TORCs and Akt. Dev Cell. 2007; 12:487–502.
25. Osaki M, Oshimura M, Ito H. PI3 K-Akt pathway: its functions and alterations in human cancer. Apoptosis. 2004; 9:667–676. [PubMed: 15505410]
26. Peroukides S, Bravou V, Alexopoulos A, Varakis J, Kalofonos H, Papadaki H. Survivin overexpression in HCC and liver cirrhosis differentially correlates with p-STAT3 and E-cadherin. Histol. Histopathol. 2010; 25:299–307. [PubMed: 20054802]

27. Montorsi M, Maggioni M, Falleni M, Pellegrini C, Donadon M, Torzilli G, Santambrogio R, Spinelli A, Coggi G, Bosari S. Survivin gene expression in chronic liver disease and hepatocellular carcinoma. Hepatogastroenterology. 2007; 54:2040–2044. [PubMed: 18251156]
28. Li P, Du Q, Cao Z, Guo Z, Evankovich J, Yan W, Chang Y, Shao L, Stolz DB, Tsung A, Geller DA. Interferon-gamma induces autophagy with growth inhibition and cell death in human hepatocellular carcinoma (HCC) cells through interferon-regulatory factor-1 (IRF-1). Cancer Lett. 2012; 314:213–222. [PubMed: 22056812]
29. Wang KK, Posmantur R, Nath R, McGinnis K, Whitton M, Talanian RV, Glantz SB, Morrow JS. Simultaneous degradation of alpha II- and beta II-spectrin by caspase 3 (CPP32) in apoptotic cells. J. Biol. Chem. 1998; 273:22490–22497. [PubMed: 9712874]
30. Danial NN, Korsmeyer SJ. Cell death: critical control points. Cell. 2004; 116:205–219. [PubMed: 14744432]
31. Pattingre S, Tassa A, Qu X, Garuti R, Liang XH, Mizushima N, Packer M, Schneider MD, Levine B. Bcl-2 antiapoptotic proteins inhibit Beclin 1-dependent autophagy. Cell. 2005; 122:927–939. [PubMed: 16179260]
32. Wang L, Yu C, Lu Y, He P, Guo J, Zhang C, Song Q, Ma D, Shi T, Chen Y. TMEM166, a novel transmembrane protein, regulates cell autophagy and apoptosis. Apoptosis. 2007; 12:1489–1502. [PubMed: 17492404]
33. Shamas-Din A, Brahmbhatt H, Leber B, Andrews DW. BH3-only proteins: orchestrators of apoptosis. Biochim. Biophys. Acta. 2011; 1813:508–520. [PubMed: 21146563]
34. Yang ZJ, Chee CE, Huang S, Sinicrope F. Autophagy modulation for cancer therapy. Cancer Biol. Ther. 2011; 11:169–176. [PubMed: 21263212]
35. Cheung CH, Cheng L, Chang KY, Chen HH, Chang JY. Investigations of survivin: the past, present and future. Front. Biosci. 2011; 16:952–961.
36. Vanags DM, Porn-Ares MI, Coppola S, Burgess DH, Orrenius S. Protease involvement in fodrin cleavage and phosphatidylserine exposure in apoptosis. J. Biol. Chem. 1996; 271:31075–31085. [PubMed: 8940103]
37. Nath R, Raser KJ, McGinnis K, Nadimpalli R, Stafford D, Wang KK. Effects of ICE-like protease and calpain inhibitors on neuronal apoptosis. Neuroreport. 1996; 8:249–255. [PubMed: 9051790]
38. Nath R, Raser KJ, Stafford D, Hajimohammadreza I, Posner A, Allen H, Talanian RV, Yuen P, Gilbertsen RB, Wang KK. Non-erythroid alpha-spectrin breakdown by calpain and interleukin 1 beta-converting-enzyme-like protease(s) in apoptotic cells: contributory roles of both protease families in neuronal apoptosis. Biochem. J. 1996; 319:683–690. [PubMed: 8920967]
39. Di Stasi AM, Gallo V, Ceccarini M, Petrucci TC. Neuronal fodrin proteolysis occurs independently of excitatory amino acid-induced neurotoxicity. Neuron. 1991; 6:445–454. [PubMed: 1848081]
40. Croall DE, Ersfeld K. The calpains:modular designs and functional diversity. Genome Biol. 2007; 8:218. [PubMed: 17608959]

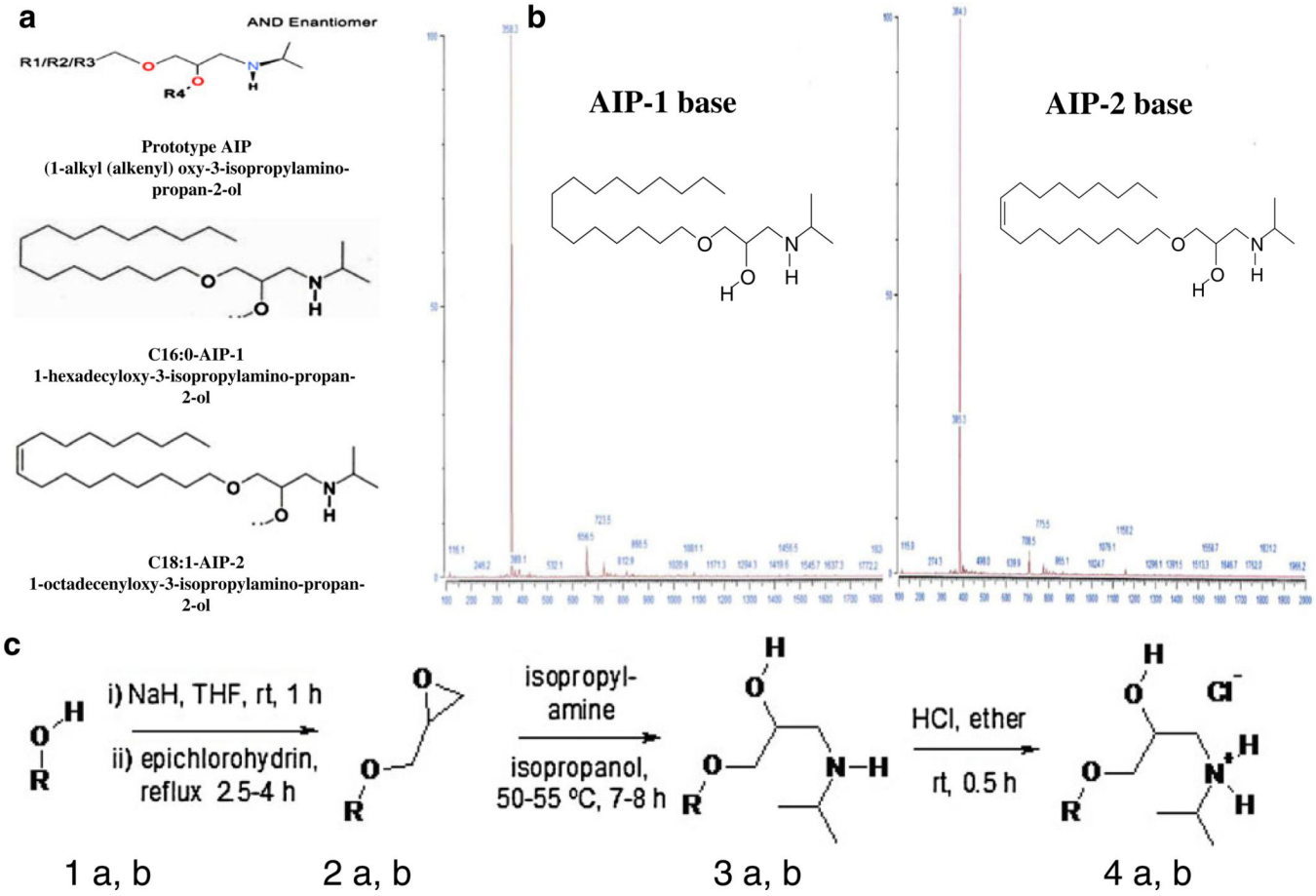


**Fig. 1.**

AIPs chemical structures, mass spectra and synthesis. a Schematic chemical structures of AIP-1 and AIP-2. b mass spectra of AIP-1 and AIP-2. c Schemes for chemical preparation of AIP compounds

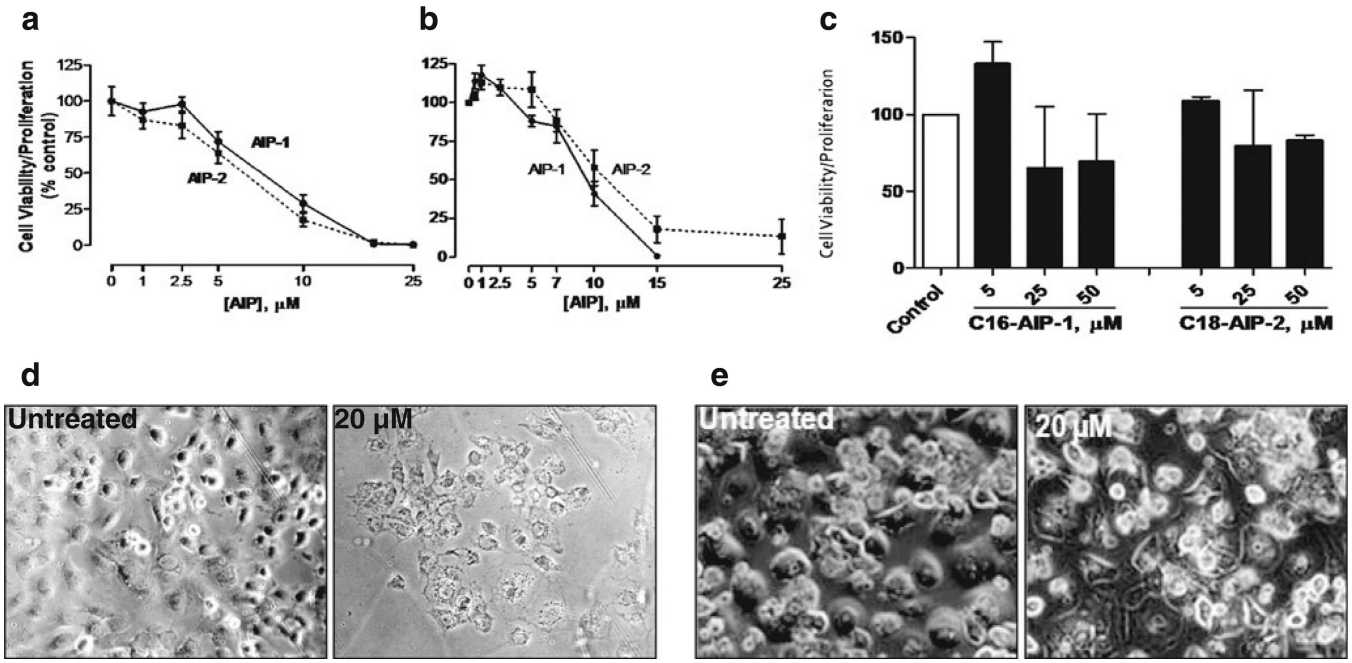


**Fig. 2.**

AIPs inhibit proliferation and viability of human and murine liver cancer cells, but not of normal human hepatocytes. Huh7 **(a)** and 1MEA (**b**) cells ($1\times10^4$/well) were seeded in 96-well flat plates and cultured in DMEM with 10 % FBS. Twelve hours later, cells were treated with different doses of AIP-1(black circle), AIP-2 (*black square*) or DMSO as a control for another 24 h. At the end of the incubation period, 20 μl of the combined MTS/PMS solution was added to each well. Following 4 h of incubation at 37 °C, formazan production was measured at 490 nm absorbance. The results are presented as means ± SD from three independent experiments. Inhibition graphs were plotted using mean values obtained from each concentration relative to control values. Normal primary human hepatocytes were cultured in DMEM/F12 (1:1) culture medium and were at least 90 % viable before treatment. c Alternatively, cells ($1\times10^5$/well) were seeded in 12-well plates and treated with or without test compounds of various concentrations in DMEM medium containing 10 % FBS. At the end of treatment, cell morphological changes were photographed using a bright field light microscope. d Huh7 treated without (*left panel*) or with (*right panel*) AIP-1 (20 μM). **e** Normal human hepatocytes treated without (*left panel*) or with (*right panel*) AIP-1 (20 μM). The data shown are representative of at least three independent experiments

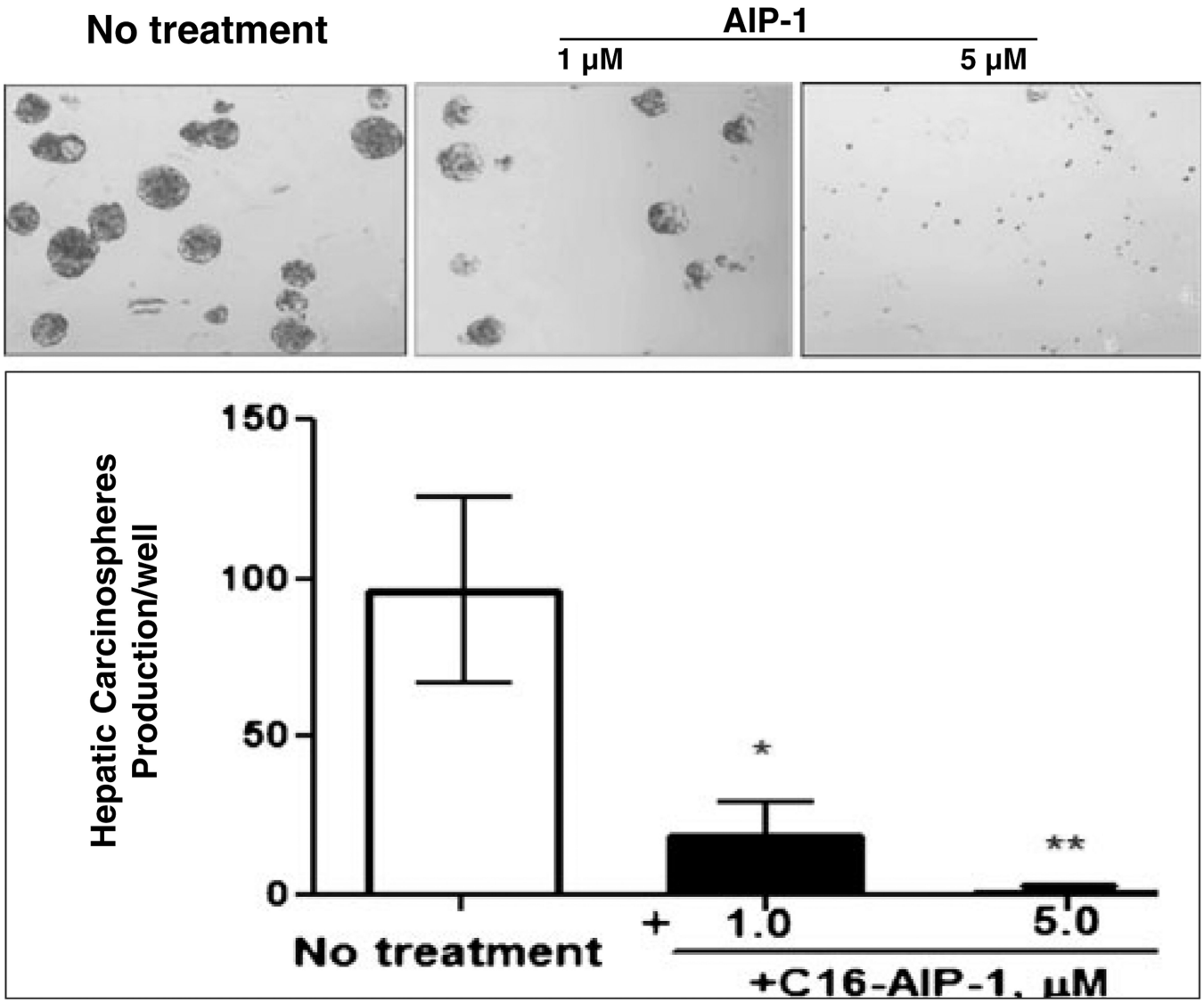


**Fig. 3.**

AIPs inhibit Huh7 carcinospheroid formation in serum-free and anchorage-free medium. Sub-confluent Huh-7 cells were collected and re-suspended in small volumes of serum-free DMEM/F12 medium, triturated and verified visually to contain only single cells, and counted in a hemocytometer. The cells were seeded in 6-well plates ($5\times10^4$ cells/well) in serum-free (DMEM)/F12 medium, 1:1 supplemented with 0.8 % methylcellulose (MC), followed by the addition of AIPs at different concentrations (1–5 μM). The sizes of the carcinospheroids were evaluated and the numbers per well were counted after 14 days using a phase contrast microscope equipped with morphometric analysis software at ×20 magnification (upper panel). Data are shown as means ± SD of values from triplicate experiments (lower panel) (*P<0.05 versus control without treatment; ** P<0.01 versus control without treatment)

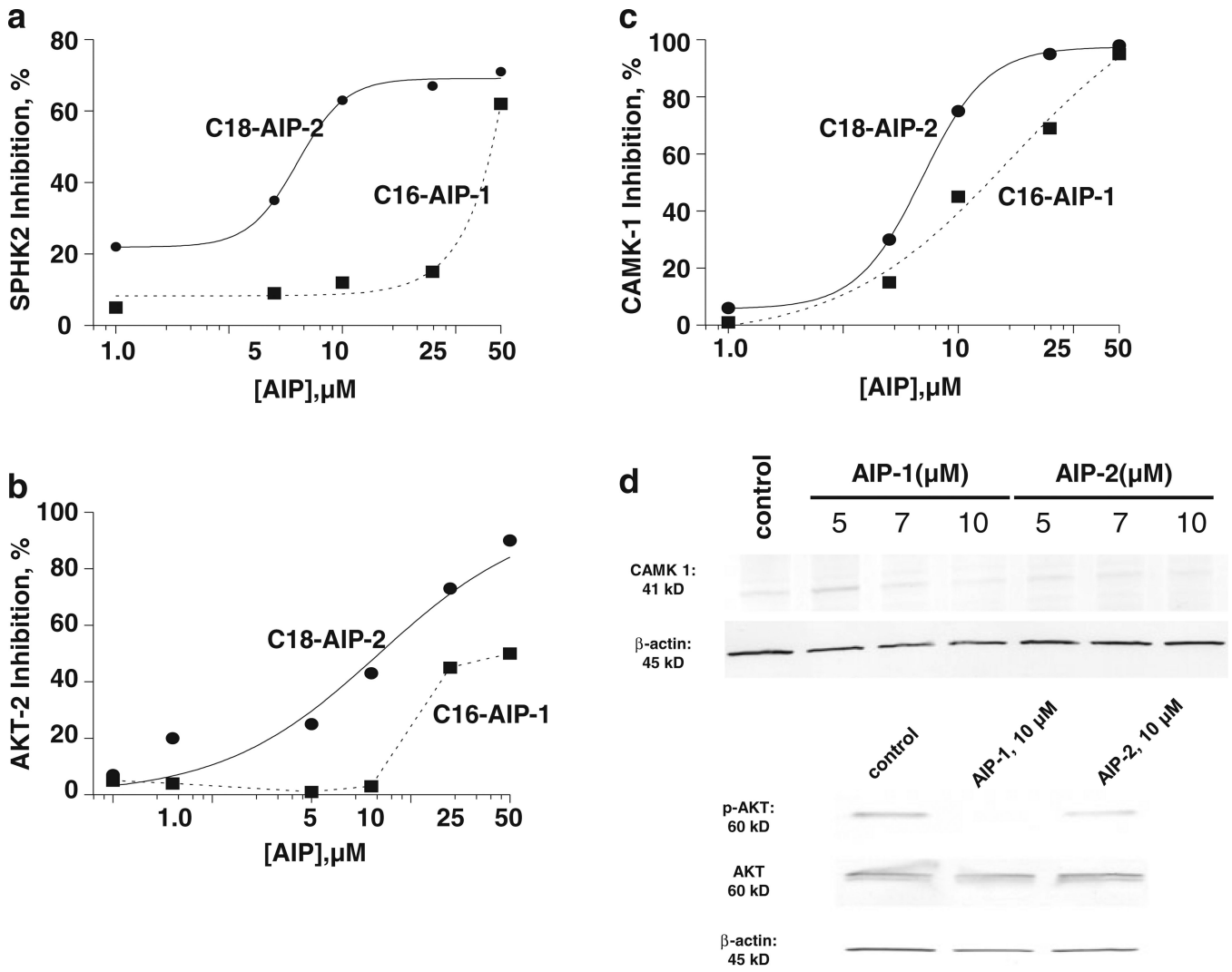


**Fig. 4.**

AIP inhibition of a selected panel of kinases in cell-free and intact Huh7 cell systems. **a**–**c** dose-dependent curves for inhibition of CAMK-1, AKT-2 and SPHK2 by AIP-1 (black circle) and AIP-2 (black square). d Inhibition of CAMK-1, AKT phosphorylation, and AKT and SPHK2 expression in Huh7 cells. Cell lysates were prepared after Huh7 cell incubation with AIP-1 and AIP-2 for 18 h, and resolved by SDS-PAGE and immunoblotted using CAMK-1, p-AKT, AKT and SPHK2 specific antibodies, respectively. β-actin was used as a loading control. The data are representative of at least three independent experiments

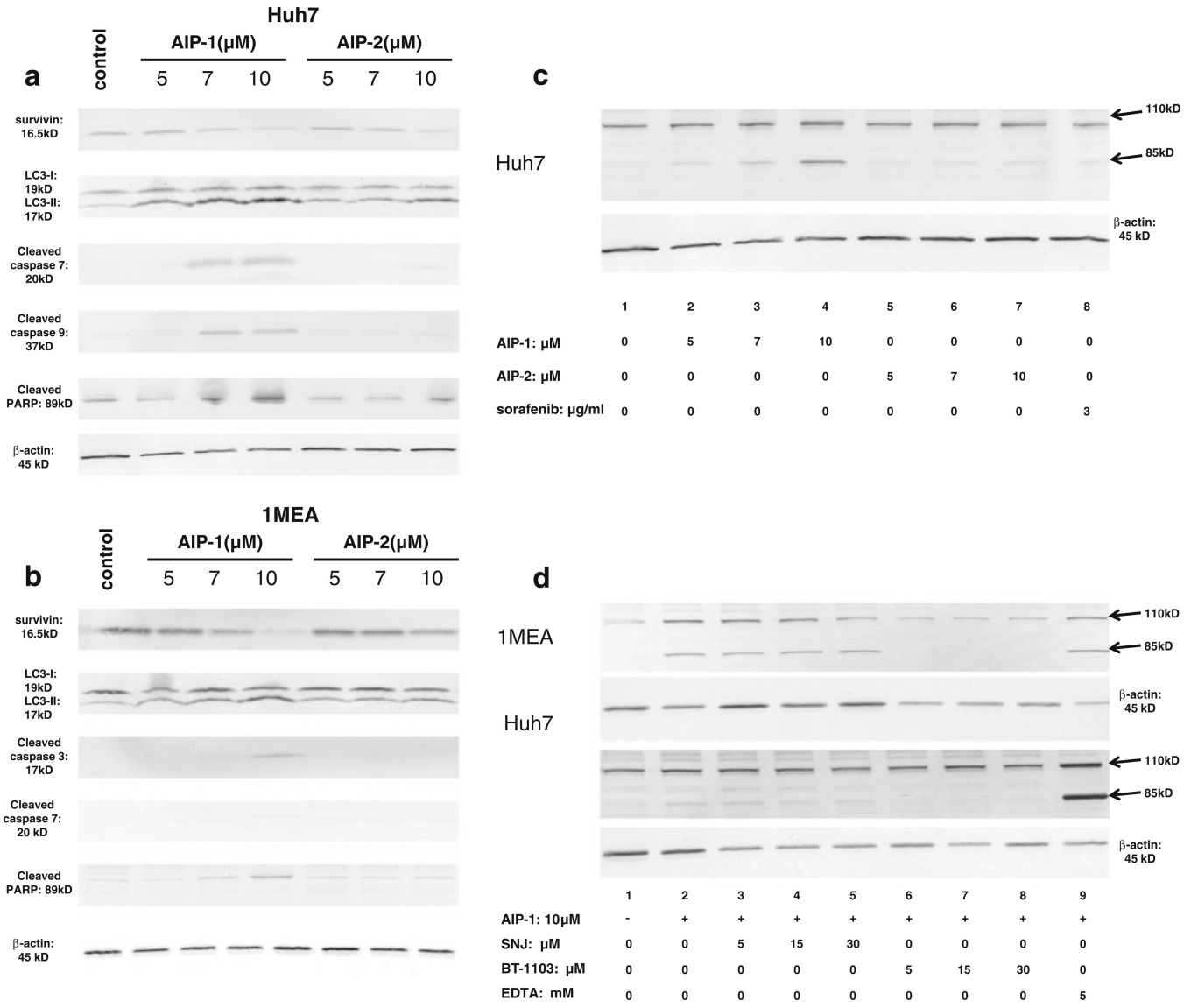


**Fig. 5.**

Apoptosis induction and beta-spectrin expression in Huh7 and 1MEA cells. **a**. Expression of survivin, LC3-I, LC3-II, cleaved caspase 7, cleaved caspase 9 and cleaved PARP in Huh7 cells treated with or without AIP-1 and AIP-2. **b** Expression of survivin, LC3-I, LC3-II, cleaved caspase 3, cleaved caspase 7 and cleaved PARP in 1MEA cells treated with or without AIP-1 and AIP-2. **c** Expression of beta-spectrin in Huh7 cells treated with or without AIP-1, AIP-2 and sorafenib. **d** After overnight culture, SNJ-1945, BT-1103 and EDTA were added to cells at different doses for 30 min, after which 10 μM AIP-1 was added. Cell lysates were resolved by SDS-PAGE and immunoblotted with a β II spectrin specific antibody. β-actin was used as a loading control. Representative Western blots are shown of β II spectrin breakdown products corresponding to 110 kD and 85 kD bands in 1MEA cells (*upper panel*) and Huh7 cells (*lower panel*)

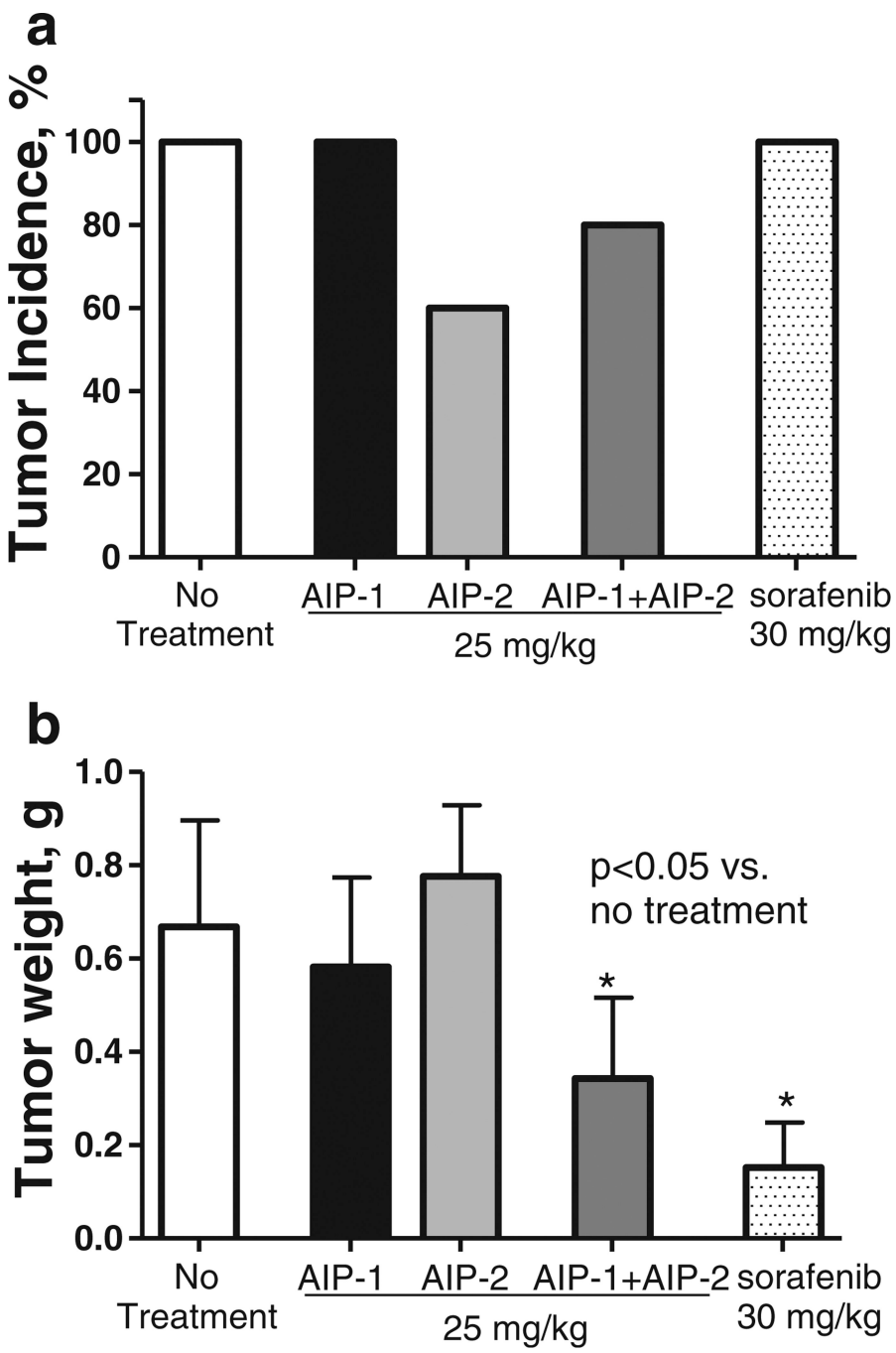


**Fig. 6.**

AIP administration inhibits liver cancer growth in an allograft tumor model. BALB/c mice (6- to 8-week old) were injected (s.c.) with 1MEA cells ($5\times10^6$/mouse). After 1 week, mice were randomly divided into five groups and orally fed with AIP-1, AIP-2, AIP-1 + AIP-2 (25 mg/kg), Sorafenib (30 mg/kg) or 100 μl PBS (control group), respectively, once daily for 5 days weekly, by gavage for 4 weeks. After that, mice were sacrificed and the tumors were recovered and weighed. a Tumor incidence (percentage of tumor-bearing mice of total tumor cell-inoculated mice). **b** Weight of tumor tissue recovered from tumor-bearing mice. Data

represent the mean ± SD from one of two similar experiments (*$P$<0.05 versus control without treatment)